What is dark matter made of?

Bruce Hoeneisen

e-mail: bhoeneisen@usfq.edu.ec

Universidad San Francisco de Quito

Presented at the 3rd World Summit on Exploring the Dark Side of the Universe
Guadeloupe Islands, March 9-13 2020

Abstract

I present an overview of detailed and redundant measurements of dark matter properties, and discuss discrepancies with current limits.

1 Introduction

At the 2020 Guadeloupe meeting I presented measurements of dark matter properties published in References [1], [2], [3], [4], and [5]. These detailed, precise and redundant measurements, summarized in Table 1 below, are in disagreement with some limits on thermal relic masses [6] [7] [8] [9]. In these Proceedings I present a short overview of the measurements, and a few comments on the disagreements.

Figure 1: Guadeloupe Islands.

2 Motivation

We assume that dark matter is a gas of particles, either fermions or bosons. As the universe expands, this gas becomes non-relativistic. We assume that these non-relativistic particles have negligible interactions with the standard model sector, and negligible inelastic self interactions, except for gravitation. Let a be the expansion parameter of the universe normalized to $a = 1$ at the present time. As the universe expands and cools, the root-mean-square (rms) velocity of the dark matter particles scales as $\propto 1/a$, and the dark matter density scales as $\propto 1/a^3$:

$$v_{h\text{rms}}(a) = \frac{v_{h\text{rms}}(1)}{a}, \qquad \rho_h(a) = \frac{\Omega_c \rho_{\text{crit}}}{a^3}. \tag{1}$$

Note that the adiabatic invariant $v_{h\text{rms}}(a)/\rho_h(a)^{1/3}$ is independent of a. (Throughout, the sub-index h stands for "dark matter halo". We use the standard notation of [10].) The adiabatic invariant remains constant if the mean number of particles per orbital remains constant.

Now consider a free observer in a density peak in the expanding universe. This observer feels no gravity. The matter in this peak expands, reaches maximum expansion, and then, due to gravitational attraction, collapses adiabatically forming the core of a galaxy. Let $\sqrt{3}\left\langle v_{rh}^2 \right\rangle^{1/2}$ be the rms velocity of dark matter particles in the galaxy (v_{rh} is the radial component), and $\rho(r \to 0)$ be the dark matter density in the core of the galaxy. Adiabatic expansion implies

$$\frac{v_{h\text{rms}}(a)}{\rho_h(a)^{1/3}} = \frac{v_{h\text{rms}}(1)}{(\Omega_c \rho_{\text{crit}})^{1/3}} = \frac{\sqrt{3}\left\langle v_{rh}^2 \right\rangle^{1/2}}{\rho(r \to 0)^{1/3}}. \tag{2}$$

The interest in Equation (2) is that we can measure both $\left\langle v_{\text{rh}}^2 \right\rangle^{1/2}$ and $\rho_h(r \to 0)$, and hence $v_{h\text{rms}}(1)$, in spiral galaxies. Furthermore, the core of spiral galaxies can have 10^8 times the mean dark matter density of the universe [3], and therefore, is a promising place to study dark matter.

In conclusion, we *predict* that the adiabatic invariant $v_{h\text{rms}}(1)$ is of cosmological origin, and therefore is the same for all relaxed, steady-state, spiral galaxies.

Fermions Observable	$v_{h\text{rms}}(1)$ [km/s]	$a'_{h\text{NR}} \times 10^6$	m_h [eV]	k_{fs} [Mpc^{-1}]	$\log_{10}(M_{\text{fs}}/M_\odot)$
Spiral galaxies	0.76 ± 0.29	2.54 ± 0.97	79^{+35}_{-17}	$0.80^{+0.42}_{-0.24}$	12.08 ± 0.50
No freeze-in/-out	$0.81^{+0.47}_{-0.25}$	$2.69^{+1.57}_{-0.84}$	75 ± 23	0.76 ± 0.31	12.14 ± 0.52
M_s distribution				$0.90^{+0.44}_{-0.34}$	11.93 ± 0.56
Bosons Observable	$v_{h\text{rms}}(1)$ [km/s]	$a'_{h\text{NR}} \times 10^6$	m_h [eV]	k_{fs} [Mpc^{-1}]	$\log_{10}(M_{\text{fs}}/M_\odot)$
Spiral galaxies	0.76 ± 0.29	2.54 ± 0.97	51^{+22}_{-11}	$0.51^{+0.28}_{-0.15}$	12.66 ± 0.50
No freeze-in/-out	$0.26^{+0.16}_{-0.08}$	$0.88^{+0.52}_{-0.28}$	113 ± 35	1.26 ± 0.50	11.49 ± 0.52
M_s distribution				$0.90^{+0.44}_{-0.34}$	11.93 ± 0.56

Table 1: Summary of three independent measurements of the adiabatic invariant $v_{h\text{rms}}(1)$ [4], the expansion parameter at which dark matter particles become non-relativistic $a'_{h\text{NR}} \equiv v_{h\text{rms}}(1)/c$, the cut-off wavenumber of warm dark matter k_{fs}, the transition galaxy mass M_{fs}, and the mass m_h of dark matter particles (for the case of zero chemical potential). The top (bottom) table is for fermions with $N_f = 2$ (bosons with $N_b = 1$). Update of Table 2 of Reference [4].

3 Validation

To test this prediction we study spiral galaxies in the "Spitzer Photometry and Accurate Rotation Curves" (SPARC) sample [11]. The SPARC galaxy sample includes a very broad range of lumi-

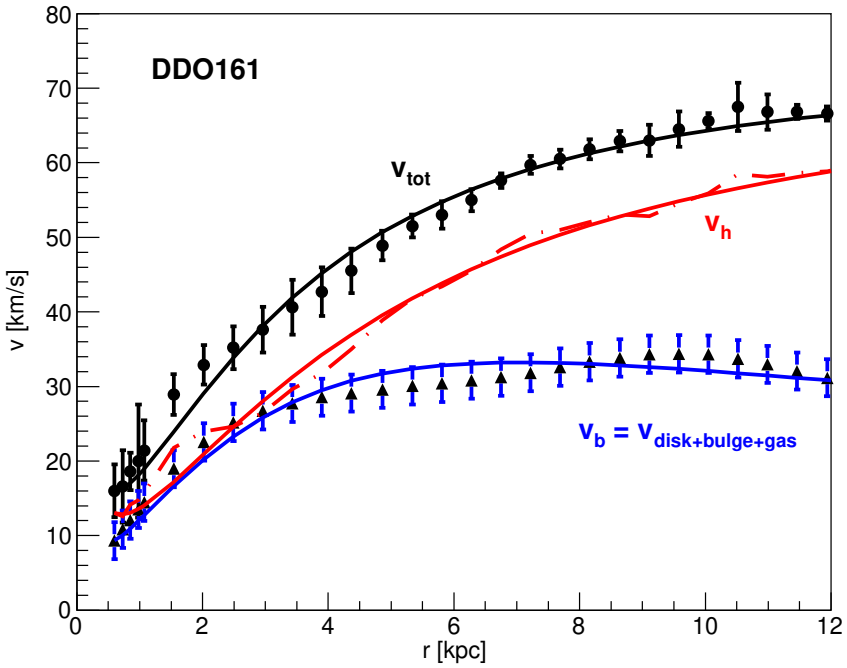

Figure 2: Observed rotation curve $v_{\rm tot}(r) \equiv v(r)$ (dots) and the baryon contribution $v_b(r)$ (triangles) of galaxy DDO161 [11]. The dot-dash line is from $v_h(r)^2 = v(r)^2 - v_b(r)^2$. The solid lines are obtained by numerical integration [1].

nosities, surface brightnesses, rotation velocities, and Hubble types. As an example, the rotation curves of galaxy DDO161 are presented in Figure 2. $v_{\rm tot}(r) \equiv v(r)$ is the velocity of rotation of a test particle in a circular orbit of radius r in the plane of the galaxy. This rotation velocity $v(r)$ has contributions from baryons (stars in the disk and bulge, and gas), and from the halo of dark matter: $v(r)^2 = v_b(r)^2 + v_h(r)^2$. The flat rotation velocity $v(r)$ at large r determines the root-mean-square (rms) of the radial component of the velocities of the dark matter particles $\langle v_{rh}^2 \rangle^{1/2} = v_{\rm flat}/\sqrt{2}$. The slopes of $v(r)$ and $v_b(r)$ at small r determine the dark matter density in the core of the galaxy: $\rho_h(r \to 0) = 3\left[v(r)^2 - v_b(r)^2\right]/(4\pi G r^2)$. So we are able to measure the adiabatic invariant (2) for each SPARC galaxy.

To take full advantage of all measured rotation velocities $v(r)$ and $v_b(r)$, we fit four boundary conditions needed to integrate differential equations describing two self-gravitating non-relativistic gases: dark matter and baryons. These numerical integrations are shown with continuous lines in Figure 2. Note that we do not fit templates. Good fits are obtained assuming that the dark matter rms velocity $\sqrt{3}\,\langle v_{rh}^2 \rangle^{1/2}$ is independent of r. This important observation implies that the velocities of dark matter particles satisfy approximately the Boltzmann distribution. How did dark matter acquire the Boltzmann distribution of velocities? Was dark matter ever in thermal equilibrium with "something"? From the rotation curves of 40 well measured, relaxed, steady-state galaxies we obtain the distribution of $v_{h\rm rms}(1)$ presented in Figure 3 [3]. This distribution has a mean 0.87 km/s, and a standard deviation of 0.27 km/s. This small relative standard deviation is noteworthy given that the galaxies in this sample have luminosities, central densities, and central surface brightnesses that span three orders of magnitude. We do not find any statistically significant dependence of $v_{h\rm rms}(1)$ on the

galaxy properties, see Table 2.

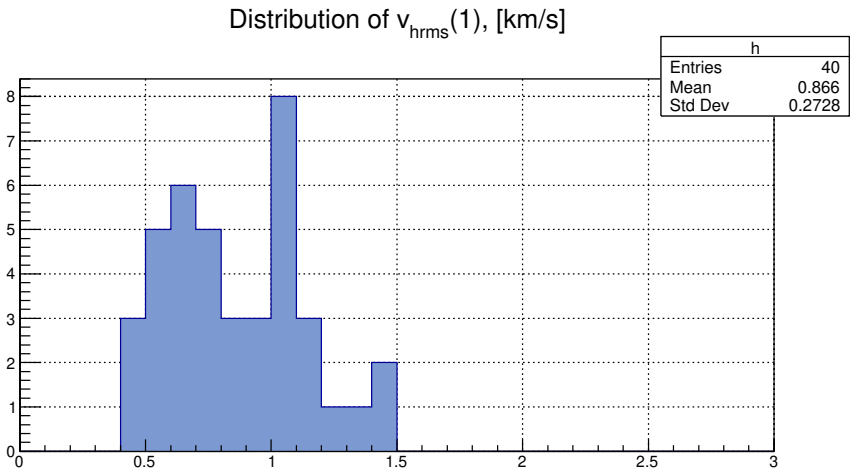

Figure 3: Distribution of the adiabatic invariant $v_{h\mathrm{rms}}(1)$ obtained from fits to rotation curves of 40 spiral galaxies in the SPARC sample [11]. Case for chemical potential $\mu \ll 0$.

From Figure 3, and a similar figure for fermions with chemical potential $\mu = 0$ [3], we take

$$v_{h\mathrm{rms}}(1) = (0.82 \pm 0.31)\sqrt{1-\kappa_h}\ \mathrm{km/s} = 0.76 \pm 0.29\ \mathrm{km/s}. \tag{3}$$

The factor $\sqrt{1-\kappa_h}$ is a correction for possible dark matter rotation. We take $\kappa = 0.15 \pm 0.15$ [1] [2] [3]. This range is also consistent with $v_{h\mathrm{rms}}(1)$ obtained from 10 different galaxies in the THINGS sample [2] [12].

Galaxy selection	N	Mean $v_{h\mathrm{rms}}(1)$ [km/s]	Std. dev. [km/s]
All	40	0.866	0.273
$L_{3.6} < 1 \times 10^9 L_\odot$	11	0.838	0.297
$L_{3.6} > 4 \times 10^9 L_\odot$	11	1.036	0.192
$M_{HI} < 1 \times 10^9 M_\odot$	17	0.714	0.239
$\langle v_{rh}^2 \rangle^{1/2} < 50$ km/s	17	0.786	0.259
$\langle v_{rh}^2 \rangle^{1/2} > 60$ km/s	16	0.969	0.227
de Vaucouleurs class 5, 6 or 7	15	0.820	0.277
de Vaucouleurs class 9 or 10	18	0.869	0.258
SBdisk $< 100 \times 10^9 L_\odot/\mathrm{pc}^2$	10	0.843	0.174
$\rho_h(0) > \rho_b(0)$	37	0.842	0.255

Table 2: Mean and standard deviation of $v_{h\mathrm{rms}}(1)$ for several galaxy selections [3]. N is the number of galaxies in the selection. $L_{3.6}$ is the absolute luminosity at 3.6 μm. M_{HI} is the mass of atomic hydrogen gas (HI). "SBdisk" is the Disk Central Surface Brightness at 3.6 μm. The galaxy classes are 5 = Sc, 6 = Scd, 7 = Sd, 9 = Sm, 10 = Im. The data is from the SPARC sample of spiral galaxies [11].

In conclusion, we observe that, within experimental uncertainties, the "adiabatic invariant" $v_{h\mathrm{rms}}(1)$ is approximately the same for all relaxed, steady-state, galaxies in our sample. This observation suggests that $v_{h\mathrm{rms}}(1)$ is indeed of cosmological origin.

We define $a'_{h\text{NR}} \equiv v_{h\text{rms}}(1)/c$. Dark matter is ultra-relativistic for $a \ll a'_{h\text{NR}}$, and non-relativistic for $a \gg a'_{h\text{NR}}$. Note that the mass of matter inside the horizon at $a = a'_{h\text{NR}}$ is $\approx 3 \times 10^{11} M_\odot$, not much smaller than the Milky Way mass. Is this a coincidence?

4 Lower bounds to the dark matter particle mass m_h

As we lower the dark matter particle mass m_h in the fits to the observed spiral galaxy rotation curves, we obtain disagreement due to the onset of Fermi-Dirac or Bose-Einstein degeneracy in the galaxy core. This disagreement sets lower bounds to m_h of 16 eV for fermions, and 45 eV for bosons, at 99 % confidence [1]. These limits exclude Einstein condensation, and exclude full fermion degeneracy. Chemical potential $\mu \leq 0$ is allowed for both fermions and bosons.

5 Why a core and not a cusp?

Consider galaxy UGC11914. The measured dark matter density in the core $\rho_h(r \to 0)$ is $(2.1 \pm 0.5) \times 10^8$ times the mean dark matter density of the universe $\Omega_c \rho_{\text{crit}}$ [3]! What prevented dark matter from collapsing to infinite density as suggested by simulations in the cold dark matter ΛCDM scenario? Why a core and not a cusp? The answer: a galaxy with a given $v_{\text{flat}} = \sqrt{2} \left\langle v_{rh}^2 \right\rangle^{1/2}$ has a well defined dark matter density in the core $\rho_h(r \to 0)$ given by Equation (2).

6 Free-streaming

Let $P(k)$ be the power spectrum of linear density perturbations in the cold dark matter ΛCDM model. k is the comoving wavenumber. If dark matter is warm, the power spectrum becomes $P(k)\tau^2(k/k_{\text{fs}})$, where $\tau^2(k/k_{\text{fs}})$ is a cut-off factor due to dark matter free-streaming. We use the approximation $\tau^2(k/k_{\text{fs}}) = \exp\left(-k^2/k_{\text{fs}}^2\right)$ [5]. The cut-off wavenumber k_{fs} can be calculated from $a'_{h\text{NR}}$, see Reference [4]. We obtain $k_{\text{fs}} = 0.80^{+0.42}_{-0.24}$ Mpc^{-1}. The halo "transition" mass, corresponding to a gaussian cut-off factor, is defined to be $M_{\text{fs}} \equiv 4\pi(1.555/k_{\text{fs}})^3 \Omega_m \rho_{\text{crit}}/3$. Results derived from Equation (3) are presented in Table 1. Note that the measured M_{fs} is similar to the Milky Way mass, and hence addresses the "small scale crisis" problems.

7 Measurement of the cut-off wavenumber with galaxy stellar mass distributions

Figure 4 compares galaxy stellar mass distribution predictions with observations at $z \approx 4.5$. The cold and warm dark matter models coincide for halo masses $M_h > M_{\text{fs}}$, and differ for $M_h < M_{\text{fs}}$. Therefore, to measure the cut-off wavenumber k_{fs}, we first adjust the relation between the halo mass M_h and the stellar mass M_s to obtain agreement for $M_h > M_{\text{fs}}$, and obtain $\log_{10}(M_s/M_h) = -1.5$, consistent with Figure 9 of Reference [13]. From Figure 4, and similar figures at $z = 6$, 7, and 8, we obtain $k_{\text{fs}} = 0.90^{+0.44}_{-0.34}$ Mpc^{-1} [5]. The agreement with the value of k_{fs} obtained in Section 6 is evidence that k_{fs} is indeed due to free-streaming, and confirms, once again, that $v_{h\text{rms}}(1)$ is of cosmological origin.

8 Warm dark matter with no freeze-in and no freeze-out

The measurements of $v_{h\text{rms}}(1)$, or equivalently k_{fs}, described above do not determine the dark matter particle mass m_h, only the dark matter temperature-to-mass ratio $T_h(a)/m_h$. To obtain m_h and $T_h(a)$

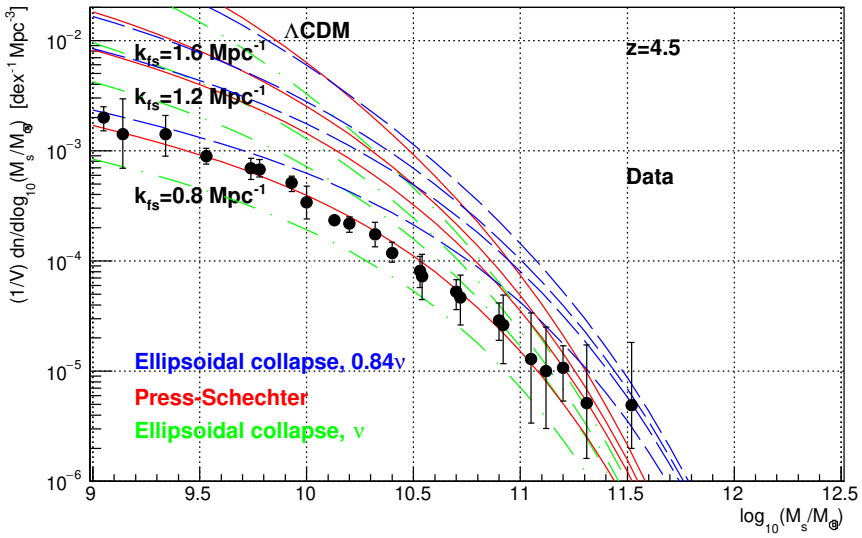

Figure 4: Calculated stellar mass functions with the Press-Schechter [14], Ellipsoidal Collapse with $\tilde{\nu} = \nu$, and Ellipsoidal Collapse with $\tilde{\nu} = 0.84\nu$ [15] [16] approximations, for ΛCDM, and ΛWDM with $k_{\rm fs} = 1.6, 1.2$, and 0.8 Mpc^{-1}, at redshift $z = 4.5$, compared with observations at $z \approx 4.5$ [13] [17] [18] [19]. $\log_{10}(M_h) = \log_{10}(M_s) + 1.5$.

separately, we need one more constraint. It turns out that if we assume that dark matter decoupled while ultra-relativistic and has zero chemical potential, then dark matter was in thermal equilibrium with the standard model sector in the early universe, *with the measured adiabatic invariant* $v_{hrms}(1)$ *and the measured cosmic microwave background radiation temperature* T_0 [1] [2] [4]. This miracle is either a coincidence, or strong evidence that dark matter was once in diffusive and thermal equilibrium with the standard model sector in the early universe, and decoupled from the standard model sector and from self annihilations while still ultra-relativistic. In other words, strong evidence that dark matter has no freeze-in and no freeze-out. The assumption of no freeze-in and no freeze-out leads to parameters presented in Table 1.

9 Comments on discrepancies with thermal relic limits

Fermion phase space density limits: Limits on fermion dark matter mass, from phase space density considerations, are obtained from a study of dwarf spheroidals (dSph) of the Milky Way [6]. From the Pauli exclusion principle the limit obtained is $m_{\rm DEG} = 0.41$ keV. Stronger limits are obtained with additional assumptions, e.g. the Tremaine-Gunn limit. These limits assume that dwarf spheroids are dominated by dark matter. However, at this 2020 Guadeloupe meeting, Francois Hammer presented evidence that dwarf spheroids have negligible amounts of dark matter [20], [21], [22], [23], so these limits need to be revised. In Section 4 above we present the corresponding limits from spiral galaxy rotation curves.

The UV luminosity function limit: We comment on Reference [8]. The analysis in [8] is very similar to our analysis in [5]. The conclusions, however, are quite different. In [5] we obtain excellent agreement with observations, see Figure 4, while [8] obtains a limit on the thermal relic mass $m_h \geq 2.4$ keV at 2σ.

There are three differences between these analysis: 1) The cut-off function in [8] has the form

$\tau^2 = \left[1 + (\alpha k)^{2\mu}\right]^{-10/\mu}$, originally derived in [24]. This functional form is numerically the same as our gaussian cut-off function for all practical purposes. The values of α, and the equivalent $k_{\rm fs}$'s, for several early thermal relic masses, are presented in Table 3. The values of $k_{\rm fs}$ used in [5], calculated with the method outlined in [4], is also presented in the Table. 2) To calculate the variance $\sigma^2(M, z)$, needed by the Press-Schechter calculation of the galaxy mass distribution, Reference [8] uses the top-hat window function in k-space, while in [5] we use the gaussian window function. The "knee" between the asymptotes for $k \ll k_{\rm fs}$ and $k \gg k_{\rm fs}$ is more pronounced in the former, and more rounded in the latter analysis. However, neither 1) nor 2) can account for the very different conclusions. 3) The main source of difference between the two analysis appears to be the different approximations for $P(k)$. The analysis in [5] uses Eq. (8.1.42) of Reference [25] with the astrophysical parameters in [10]. This approximation to $P(k)$ is valid for all k, so normalizing $P(k)$ to the measured σ_8 is accurate, and coincides with the Planck normalization in [10]. Reference [8] does not specify the approximation used for $P(k)$, and obtains a steeper slope in Figure 1 of [8] at large M than we do.

m_h	$1/\alpha$ [8]	$k_{\rm fs}$ [8]	$k_{\rm fs}$ [5][4]	k_J
3000 eV	48.5 Mpc^{-1}	18.9 Mpc^{-1}	20.9 Mpc^{-1}	39.6 Mpc^{-1}
1000 eV	14.3 Mpc^{-1}	5.59 Mpc^{-1}	7.8 Mpc^{-1}	13.2 Mpc^{-1}
79 eV	0.86 Mpc^{-1} *	0.33 Mpc^{-1} *	0.86 Mpc^{-1}	1.04 Mpc^{-1}

Table 3: Relation between the early thermal relic mass m_h, and the corresponding free-streaming cut-off wavenumber $k_{\rm fs}$, obtained by the methods described in References [8], and [5][4]. Also shown is the Jeans wavenumber k_J: modes with $k < k_J$ grow due to gravity, modes with $k > k_J$ are damped due to free-streaming. * Out of range?

Lyman-α forest limits: The Lyman-α forest allows measurements of the neutral hydrogen density profile along the line of sight to far away quasars (at redshifts $z \approx 5.5$). From the analysis of these density profiles, with model dependent simulations of the inter-galactic medium (including the highly ionized hydrogen), the cut-off wavenumber $k_{\rm fs}$ is excluded in the range from ≈ 0.4 Mpc^{-1} to ≈ 27 Mpc^{-1} [7]. In comparison, the measured galaxy stellar mass distributions presented in [5] obtain $k_{\rm fs} = 0.90^{+0.44}_{-0.34}$ Mpc^{-1} [5]. So, these two analysis, based on very different *data* sets, are incompatible. This discrepancy needs to be resolved.

Limits from quasar gravitational lensing: We consider Reference [9]. Strong lensing with multiple images often have anomalous flux ratios between the images. The anomaly may be due to halos with mass in the range $10^6 M_\odot$ to $10^8 M_\odot$ along the line of sight [9]. To constrain $k_{\rm fs}$ it is necessary to predict the halo mass function in the mass range $10^6 M_\odot$ to $10^8 M_\odot$ at redshifts $z < 3$. Do we really know how to predict the halo mass function at these low masses and redshifts where the Press-Schechter formalisms is already saturated [5]? Note that the Press-Schechter method, and its Sheth-Tormen modification, can only be used so long as the fraction of mass locked up in halos with mass greater than M, $F(M, z)$, is less than approximately 0.01. If $F(M, z) > 0.01$, a "would be galaxy of mass M" may "not fit", will loose mass to neighboring galaxies, and will collapse as a halo with mass $< M$ [4]. At $z < 3$, the Press-Schechter method for halos of mass $M < 10^{12} M_\odot$ is already saturated, and does not predict correctly the galaxy mass function [5].

10 Extension of the Standard Model

An integration of the Boltzmann equation for the production of sterile Majorana neutrinos after Electroweak Symmetry Breaking (when sterile and active neutrinos acquire mass and couple together) is presented in Figure 5. This example is consistent with the measurements presented in Table 1. Such sterile Majorana neutrinos evade all current (and future?) dark matter searches, and are consistent with Big Bang Nucleosynthesis.

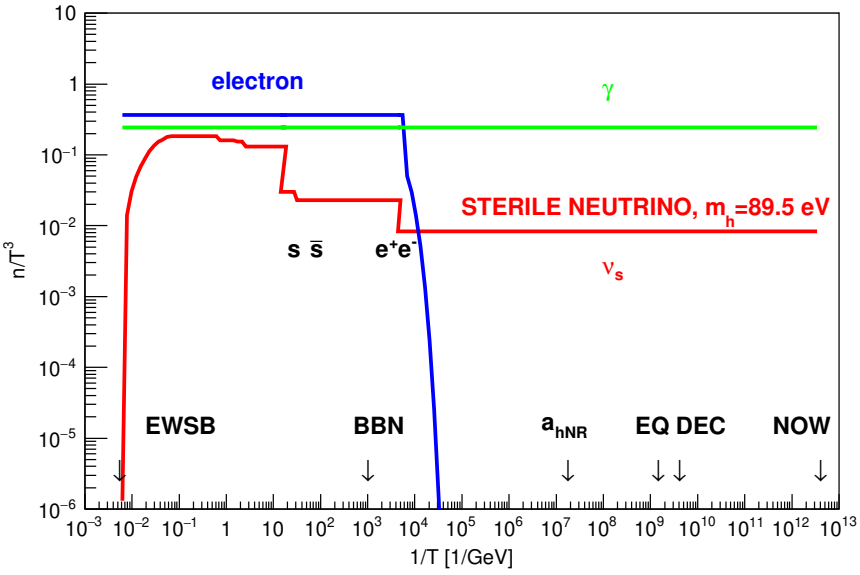

Figure 5: Example. Number density n of photons, electrons, and Majorana sterile neutrino dark matter particles with $m_h = 89.5$ eV, divided by T^3, as a function of $1/T$. T is the photon temperature. The lifetime of this sterile Majorana neutrino is 7×10^{27} yr. Big Bang Nucleosynthesis (BBN) is satisfied. From Reference [1].

11 Conclusions

We have presented detailed, precise, and redundant *measurements* of dark matter properties, that do not depend on any particular extension of the standard model, see Table 1. These measurements result in several "miracles": 1) the adiabatic invariant $v_{h\mathrm{rms}}(1)$ is the same, within experimental uncertainties, for 50 measured spiral galaxies, indicating that $v_{h\mathrm{rms}}(1)$ is of cosmological origin; 2) the measured $v_{h\mathrm{rms}}(1)$ obtains k_{fs} in agreement with k_{fs} obtained from the galaxy stellar mass functions, demonstrating that k_{fs} is due to free-streaming and $v_{h\mathrm{rms}}(1)$ is of cosmological origin; 3) the measured $v_{h\mathrm{rms}}(1)$ is consistent with no freeze-in and no freeze-out; 4) the measured transition mass M_{fs} is similar to the Milky Way mass, and so addresses the "small scale crisis"; 5) the mass of matter inside the horizon at $a'_{h\mathrm{NR}}$ is $\approx 3 \times 10^{11} M_{\odot}$, not much less than the Milky Way mass. Are these "miracles" coincidences, or are they suggesting that these measurements are indeed correct? In conclusion, these measurements should be taken seriously, and the disagreements with limits need to be resolved. Nature will have the last word.

Acknowledgements

I thank Pierre Petroff and the sponsors for a most interesting and dramatic meeting: not easy getting back home with the world falling apart!

References

[1] Hoeneisen, B. (2019) A Study of Dark Matter with Spiral Galaxy Rotation Curves. *International Journal of Astronomy and Astrophysics*, **9**, 71-96.

[2] Hoeneisen, B. (2019) A Study of Dark Matter with Spiral Galaxy Rotation Curves. Part II. *International Journal of Astronomy and Astrophysics*, **9**, 133-141.

[3] Hoeneisen, B. (2019) The adiabatic invariant of dark matter in spiral galaxies. *International Journal of Astronomy and Astrophysics*, **9**, 355-367.

[4] Hoeneisen, B. (2019) Simulations and Measurements of Warm Dark Matter Free-Streaming and Mass. *International Journal of Astronomy and Astrophysics*, **9**, 368-392. https://doi.org/10.4236/ijaa.2019.94026

[5] Hoeneisen, B. (2020) Cold or Warm Dark Matter?: A Study of Galaxy Stellar Mass Distributions *International Journal of Astronomy and Astrophysics*, **10**, 57-70. https://doi.org/10.4236/ijaa.2020.102005

[6] Boyarsky, A., Ruchayskiyc, O., and Iakubovskyi, D. (2009) A lower bound on the mass of Dark Matter particles, https://arxiv.org/abs/0808.3902

[7] Baur, J., *et al.* (2016) Lyman-alpha Forests cool WarmDark Matter https://arxiv.org/pdf/1512.01981.pdf

[8] Menci N., Grazian A., Castellano M., Sanchez N.G. (2016) A Stringent Limit on the Warm Dark Matter Particle Masses from the Abundance of z=6 Galaxies in the Hubble Frontier Fields

[9] M. Miranda, A.V. Macciò (2007) Constraining Warm Dark Matter using QSO gravitational lensing, Mon. Not. R. Astron. Soc.000, 000–000 (2007), https://arxiv.org/pdf/0706.0896.pdf

[10] Tanabashi, M., *et al.*, (Particle Data Group) (2018) The Review of Particle Physics. *Physical Review* D, **98**, Article ID: 030001.

[11] Lelli F., McGaugh S. S., Schombert (2016), SPARC: Mass models for 175 disk galaxies with Spitzer Photometry and Accurate Rotation Curves *The Astronomical Journal*, 152:157. doi:10.3847/0004-6256/152/6/157 The data in digital form is publicly available in files SPARC_Lelli2016c.mrt and LTG_data.txt.

[12] de Blok, W.J.G., *et al.* (2008), High-Resolution Rotation Curves and Galaxy Mass Models from THINGS. *The Astronomical Journal*, **136**, 2648-2719.

[13] Lapi, A. *et al.* (2017) Stellar mass function of active and quiescent galaxies via the continuity equation, https://arxiv.org/pdf/1708.07643.pdf

[14] Press, W.H., and Schechter, P. (1974) Formation of galaxies and clusters of galaxies by self-similar gravitational condensation. *The Astrophysical Journal*, **187**, 425-438.

[15] Sheth R.K., Tormen G., (1999) Large-scale bias and the peak background split, Mon. Not. R. Astron. Soc., **308**, 119-126

[16] Sheth, R.K., Mo, H.J., Tormen, G. (2001), Ellipsoidal collapse and an improved model for the number and spatial distribution of dark matter haloes, Mon. Not. R. Astron. Soc. **323**, 1-12

[17] Song, M., Finkelstein, S. L., Ashby, M. L. N., *et al.* (2016) The Evolution of the Galaxy Stellar Mass Function at $z = 4$ - 8: A Steepening Low-mass-end Slope with Increasing Redshift, ApJ, **825**, 5

[18] Grazian, A., Fontana, A., Santini, P., *et al.* (2015) The galaxy stellar mass function at $3.5 \leq z \leq 7.5$ in the CANDELS/UDS, GOODS-South, and HUDF fields, A & A, **575**, A96

[19] Davidzon, I., Ilbert, O., Laigle, C., *et al.* (2017) The COSMOS2015 galaxy stellar mass function: 13 billion years of stellar mass assembly in 10 snapshots, ApJ, in press, arXiv:1701.02734

[20] Hammer, F., Yang, Y. B., Arenou, F., Puech, M., Flores, H., Babusiaux, C., (2019) On the absence of dark matter in dwarf galaxies surrounding the Milky Way. ApJ, 883, 171

[21] Hammer, F., Yang Y., Arenou F., Wang J., Li H., Bonifacio P., and Babusiaux, C. (2020) Orbital Evidences for Dark-matter-free Milky Way Dwarf Spheroidal Galaxies.

[22] Yang Y., Hammer F., Fouquet S., Flores H., Puech M., Pawlowski M.S., and Kroupa P. (2014) Reproducing properties of MW dSphs as descendants of DM-free TDGs. MNRAS442,2419–2433

[23] Hammer F., Yang Y. B., Arenou, F., Babusiaux, C., PuechM., Flores H., (2018), Galactic Forces Rule the Dynamics of Milky Way Dwarf Galaxies. ApJ, 860, 76

[24] Bode, P., Ostriker, J.P., Turok, N. (2001) Halo Formation in Warm Dark Matter Models. *The Astrophysical Journal*, 556, 93

[25] Steven Weinberg, Cosmology, Oxford University Press (2008)